Friction **3**(3): 243–255 (2015)
DOI 10.1007/s40544-015-0090-6
ISSN 2223-7690
CN 10-1237/TH

RESEARCH ARTICLE

Elastohydrodynamic lubrication properties and friction behaviors of several ester base stocks

Yifeng HE[1,2], Thomas J. ZOLPER[3], Pinzhi LIU[2], Yuzhen ZHAO[2,4], Xingliang HE[2], Xuejin SHEN[2,5], Hongwei SUN[1], Qinghua DUAN[1], Qian WANG[2,*]

[1] *Research Institute of Petroleum Processing, SINOPEC, Beijing 100083, China*

[2] *Department of Mechanical Engineering, Northwestern University, Evanston IL 60208, USA*

[3] *Department of Mechanical Engineering, University of Wisconsin, Platteville WI 53818, USA*

[4] *Chongqing Branch of Lubricant Company, SINOPEC, Chongqing 400039, China*

[5] *School of Mechatronic Engineering and Automation, Shanghai University, Shanghai 200072, China*

Received: 19 May 2015 / Revised: 22 August 2015 / Accepted: 31 August 2015

Abstract: This paper reports a series of studies on the lubricant properties, elastohydrodynamic film thickness, and coefficients of friction of several commercially available ester base stocks, i.e., diisooctyl phthalate (DIOP), diisodecyl phthalate (DIDP), diisotridecyl phthalate (DITDP), diisooctyl sebacate (DOS), diisotridecyl sebacate (DTDS), trihydroxymethylpropyl trioleate (TMPTO), and pentaerythritol tetraoleate (PETO). The results include densities and viscosities from 303 to 398 K, and elastohydrodynamic lubricant film thicknesses and friction in the boundary, mixed and full-film lubrication regimes measured at several temperatures, loads, and speeds. These ester base stocks have different lubrication abilities owing to their chain lengths, geometric configurations, and molecular rigidity. This study provides quantitative insight into the use of ester-based lubricants for low friction through the entire lubrication regime (boundary to full film) by utilization of suitable type and size of the ester base stocks.

Keywords: ester; viscosity; elastohydrodynamic lubrication; friction; synthetic base stocks

1 Introduction

Synthetic lubricants have received much attention for their beneficial properties, such as good low- and high-temperature viscosity performance at extreme service temperatures, high thermal and oxidative stabilities, and optimal rheological-tribological properties for extensive applications. Several fully synthetic base fluids, polyalphaolefins (PAOs), polyisobutylenes (PIBs), polyalkylene glycols (PAGs), phosphate esters, alkyl benzenes, alkylated naphthalenes, fluorinated polyethers, silicones, and esters, have found wide applications in lubrication of modern machinery.

PAOs are among the most commonly used synthetic lubricating oils; they consist of hydrogenated olefin oligomers in a general formula of C_nH_{2n+2}. PAOs generally have better thermal stability of viscosity, and lower pour points and vapor pressures than their mineral oil counterparts [1]. PIBs are often used as viscosity modifiers for other base fluids to reach a high viscosity. Although PAGs have high viscosity indices, good thermal stability and excellent lubrication properties, they may dissolve certain paints and seal materials, and have compatibility problems with some nonpolar minerals and PAOs. Phosphate esters have been specially designated as fire-resistant hydraulic fluids; however they may easily degrade in an aquatic environment. Alkyl benzenes and alkylated naphthalenes can be used as additives in other base fluids to improve solubility or as the sole base fluids for certain high-temperature lubrication and heat-transfer

* Corresponding author: Qian WANG.
E-mail: qwang@northwestern.edu

applications. Fluorinated polyethers have low reactivity with other chemicals and are therefore, suitable for use under very high temperatures and in very oxidative or chemically active environments. However, cost is a significant factor restricting their wider applications. Silicones are relatively expensive, but they have poor lubrication properties and solubility in almost all other types of lubricants although they have exceptional thermal and oxidative stability, low surface tension, biological inert, and high viscosity indices [2, 3].

No matter how good the above-mentioned fluids are in certain functions, they incur some undesirable environmental and health concerns, such as poor biodegradability or toxicity to wildlife and humans [4]. Fortunately, esters, which include monoesters, diesters, phthalates, and polyol esters, have great biodegradability and benign to the environment and wildlife in case of accidental leakage or spill. In addition, they are easily synthesized without waste and sediment. Their high viscosity indices, exceptionally stable low- and high-temperature performances, and excellent lubrication properties make them preferred choices for the base oils for aircraft engine lubricants, high flash-point hydraulic fluids, and low pour-point additives for various types of lubricants.

One of the most important properties of lubricants is their oil film forming ability. The high Hertzian pressures in many tribological interfaces can cause elastic deformation and flattening of asperities in the regime of elastohydrodynamic lubrication (EHL) and mixed lubrication, which can occur in gears, rolling element bearings, cams and followers, continuously variable speed drives, and rail-wheel contacts, etc [5, 6]. The optical film thickness measurement is widely employed to evaluate the lubrication properties of a fluid via measuring EHL film thickness [7–10]. On the other hand, knowing the properties of a lubricant, the EHL film thickness, h, can be calculated by equations like the Hamrock–Dowson formula shown in Eq. (1) [11–13].

$$\frac{h}{R'} = 2.69\left(\frac{U\eta_0}{E'R'}\right)^{0.67}(\alpha^* E')^{0.53}\left(\frac{F}{E'R'^2}\right)^{-0.067}(1-0.61\mathrm{e}^{-0.73k}) \tag{1}$$

The Hamrock–Dowson equation uses a reduced radius $R' = (1/R_1+1/R_2)^{-1}$, with R_1 and R_2 the radii of curvature of the contact bodies, and an effective modulus $E' = (1-v_1^2)/E_1 + (1-v_2^2)/E_2$, with E_1 and E_2 and v_1 and v_2 the Young's moduli and Poisson's ratios of the interacting solids. Dimensionless load $W = (F/E'R'^2)$ and entrainment speed $U = (U_1 + U_2)/2$ account for kinematic interactions of the two surfaces. Meanwhile, dynamic viscosity η^0 and pressure-viscosity index α^* of the lubricant, are taken at the prevailing inlet temperature. Non-circular contacts are described by the ellipticity k.

EHL film thickness investigations for many PAOs and silicones have been conducted systematically [5, 14–22]. However, not much has been done for both natural and synthetic esters. Chang et al. employed an infrared emission technique to measure surface temperatures in an EHL contact and thence to determine the shear stress profile of several ester lubricant films [23]. Fernández et al. evaluated the influence of load and the type of lubricant on the thickness of the elastohydrodynamic film and the rolling-contact fatigue lives of AISI 52100 steel balls [24]. Höglund investigated influence of lubricant properties of several oils on elastohydrodynamic lubrication and performed a numerical EHL analysis based on the experimental data [6]. Yokoyama and Spikes explored the film-forming properties of polyol esters, polyphenyl ethers, and their mixtures over a wide range of temperature [25]. Larsson et al. studied a few base fluid parameters for elastohydrodynamic lubrication and friction calculations, and investigated their influences on lubrication capability [26]. Lord and Larsson reported the effects of slide-roll ratio and lubricant properties of a synthetic ester VG46 on elastohydrodynamic lubrication film thickness and traction, and suggested that the ester maintained a relatively thicker lubricant film during sliding than did the corresponding polyalphaolefin and mineral oils [27]. Biresaw et al. tested the elastohydrodynamic properties of a number of biobased oils [28, 29]. Bantchev et al. studied the film-forming properties of several blends including bio-based esters [30, 31]. Sarpal et al. reported the structure–property relationships of pentaerythritol polyol esters and PAOs based on the diffusion and mobility measurement and tilt angle results [32]. However, there were few reports on how the molecular structures and types of synthetic ester

base stocks affect the elastohydrodynamic lubrication properties and friction behaviors.

This work presents a group of comparative analyses of the lubricant properties and lubrication behaviors of several general ester base stocks, i.e., diesters, triesters and tetraesters, which have different molecular masses and structures. Comparisons of film thicknesses and frictions are conducted to reveal insights into the nature of these lubricants and possibilities to design novel high-performance ester lubricants.

2 Fluids and experimental procedure

The ester base stocks studied in the present work are diisooctyl phthalate (DIOP), diisodecyl phthalate (DIDP), diisotridecyl phthalate (DITDP), diisooctyl sebacate (DOS), diisotridecyl sebacate (DTDS), trihydroxymethylpropyl trioleate (TMPTO), and pentaerythritol tetraoleate (PETO) (Fig. 1). Phthalates and sebacates are diesters, and each has two ester groups in its molecule. TMPTO and PETO are polyol esters having three and four ester groups in one molecule, respectively. Among all the above tested samples, only phthalates have a phenyl ring structure. The fluid samples were obtained from China Petrochemical Corporation (Sinopec), together with the data for molecular structure, molecular mass, pour point and flash point. Their densities and viscosities in a range of temperatures, and film thicknesses and coefficient of friction in a range of operating conditions are the targeted parameters to be obtained for cross-comparison.

2.1 Density and viscosity measurements

Density ρ and kinematic viscosity υ were measured simultaneously from 298 to 423 K using a Cannon CT-2000 constant temperature bath. The density was determined by accurate measurements of the mass and

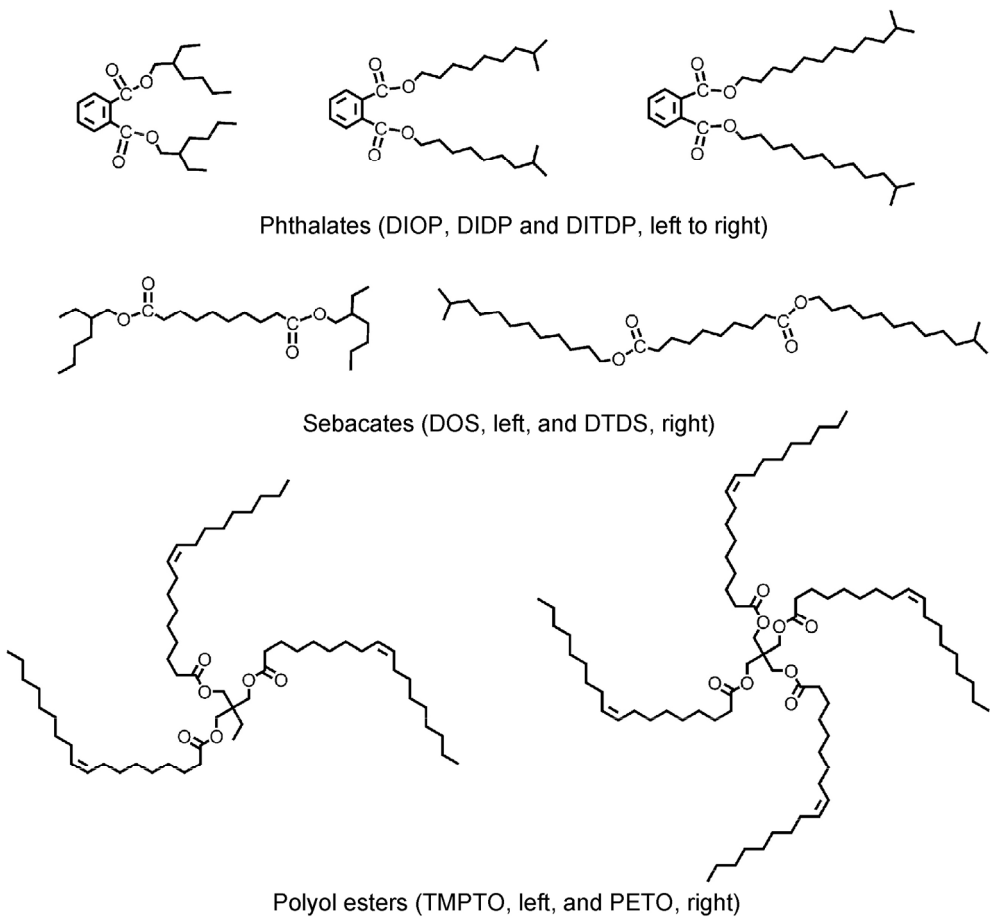

Fig. 1 Schematics of the molecular structures of base fluids, phthalates (DIOP, DIDP and DITDP), sebacates (DOS and DTDS), and polyol esters (TMPTO and PETO).

volume of each sample. The kinematic viscosity was measured using Cannon–Fenske capillary viscometers based on ASTM D 445. Multiple measurements were taken to determine the average viscosity and ensure data reproducibility. The dynamic viscosity is obtained by multiplying the measured kinematic viscosity by the density of each fluid.

2.2 Film thickness tests

Elastohydrodynamic lubricant film thickness was measured from 298 to 398 K with the method of optical interferometry between a glass disc and a steel ball using a PCS EHL ultrathin film measurement system. The system uses a polished AISI 52100 steel ball of 19.050 mm diameter, which is pressed, under 20 N load, against an optically transparent glass disk coated with a ~500 nm thick silica spacer layer. The respective Young's moduli of the glass disk and steel ball are 75 and 210 GPa, giving a maximum Hertzian pressure of 0.54 GPa [5, 22]. The root mean square (RMS) roughness values of the glass disks and steel balls are about 5 and 14 nm, respectively, giving a composite roughness of about 15 nm. This assembly is able to measure lubricant film thicknesses with a precision to 1 nm for films under 30 nm, and within 5% for film thicknesses >30 nm [13, 16]. The fluid temperature was held constant to ±1 K for each test in the temperature sequence. Before each test, the lubricant reservoir, disk, ball, and carriage were thoroughly cleaned with hexane and isopropyl alcohol solvent and allowed to dry. During the test, the ball was partly immersed in the fluid sample to allow fluid transport to the ball–disk interface.

Film thickness measurements were undertaken in nominally pure rolling conditions with the ball completely driven by the disk, with the disk velocity U_1 varying from 0.020 to 4.35 m/s. Additional measurements were made for several fluids to study shear thinning, in which the ball was attached to a separate motor-driven shaft to allow independent variation of the ball velocity U_2. This allows the slide-to-roll ratio, Σ, to vary from pure rolling ($\Sigma = 0$) to simple sliding ($\Sigma = 2$) as defined in Eq. (2).

$$\Sigma = \frac{\text{Sliding speed}}{\text{Entrainment speed}} = \left| \frac{U_1 - U_2}{(U_1 + U_2)/2} \right| \quad (2)$$

2.3 Friction tests

Friction coefficients μ were measured from 298 to 398 K using the same PCS instrument used for the film thickness studies with temperature controlled to ±1 K for each test in the temperature sequence. This portion of the studies employed 19.050 mm diameter AISI 52100 steel balls and steel disks, each pair placed under the same 20 N load. The Young's moduli of the steel disk and steel ball are both 210 GPa, giving a maximum Hertzian pressure of 0.82 GPa. The surface roughnesses of the balls and disks were about 5 and 30 nm, respectively, yielding a composite surface roughness of approximately 30 nm. The ball velocity was varied from 0.025 to 5.00 m/s. The friction measurements were done at $\Sigma = 0.50$ and $\Sigma = 1.00$ [5].

2.4 Pin-on-disk friction tests

Pin-on-disk tests were conducted to further confirm the friction behaviors of the fluids using a CETR UMT-2 tribometer, which consists of a rotating disk (E52100 steel) and a fixed pin (M50 bearing steel ball, ∅9.53 mm). A lubricant was added in the disk reservoir. During a test, the speed was linearly changed from 1.5 mm/s to 150 mm/s at 25 °C under 3 N (~ 700 MPa of the max Hertzian contact pressure).

3 Results and discussion

3.1 Density and viscosity

Densities and viscosities of the lubricants tested at 303, 348, and 398 K are listed in Table 1. For phthalates (DIOP, DIDP and DITDP), the density decreases and the viscosity increases from DIOP to DIDP to DITDP that have similar molecular structures; but the density decreases with the increase in molecular mass, i.e., the increase in the length of hydrocarbon chain attached to the phenyl ring. The densities and viscosities of sebacates (DOS and DTDS) change similarly. Unlike these five esters, the density and viscosity of PETO are higher than those of TMPTO, owing to the extra oleate group. Both the flash and pour points of phthalates (DIOP, DIDP and DITDP) increase with the length of the side chains on the phenyl ring. The flash and pour points of sebacates (DOS and DTDS) and polyol esters

Table 1 Molecular mass, flash point, pour point, density, viscosity, activation energy, and viscosity index (VI) for ester base stocks with varying structures.

Sample	Molecular mass (g/mol)	Flash point (°C)	Pour point (°C)	Density (g/cm^3)			Viscosity (mPa·s)			Activation energy (kJ/mol)	VI
				303 K	348 K	398 K	303 K	348 K	398 K		
DIOP	391	218	–53	0.98	0.94	0.91	49.8	7.6	2.5	39.3	19
DIDP	447	232	–50	0.96	0.93	0.89	71.8	9.9	3.1	42.1	46
DITDP	531	254	–37	0.94	0.91	0.88	160.6	16.2	4.3	49.9	43
DOS	427	220	–60	0.91	0.88	0.85	15.7	4.4	1.9	24.8	134
DTDS	567	244	–55	0.90	0.87	0.84	53.7	10.4	3.7	33.6	138
TMPTO	928	300	–35	0.91	0.88	0.85	75.0	15.6	5.5	31.6	177
PETO	1194	306	–29	0.92	0.89	0.86	101.2	20.8	7.2	32.3	183

(TMPTO and PETO) also demonstrated similar trends controlled by the side chain length or number of chains.

Figure 2 plots the viscosity variation as a function of molecular mass for the lubricants studied, which clearly show the viscosity and molecular mass correlation for the lubricants of the similar molecular structures. Between sebacates and phthalates, compared with DTDS, DITDP has the same two isotridecyl groups and less molecular weight, but has a higher viscosity. An important factor for the higher viscosity of the DITDP can be attributed to the rigid phenyl ring in the structure.

The Andrade–Eyring equation (Eq. (3)) describes the temperature dependence of viscosity, where η_R is the low shear viscosity at infinite temperature, ΔG^* is the activation energy for a viscous flow, resulting from the movement of an "activated" molecule from one equilibrium position to another in the preferred direction of shear; treated as a jump over a potential-energy barrier [33]. R is the universal gas constant, and T is the operating temperature [5, 34]. The activation energy for various lubricants can be thus obtained from the viscosity data over the whole temperature range of interest through a non-linear regression, and the results are also given in Table 1.

$$\eta_0(T) = \eta_R \cdot e^{\frac{\Delta G^*}{RT}} \tag{3}$$

Activation energy generally increases with the molecule size. For example, from DIOP to DIDP and further to DITDP, the increasing length of the hydrocarbon chain attached to the phenyl ring leads to an obvious increase in ΔG^* from 39.3 kJ/mol to 49.9 kJ/mol, which exhibits a strong Arrhenius behavior (Fig. 3). DOS and DTDS also show a similar trend. However, the activation energy of PETO is very close to that of

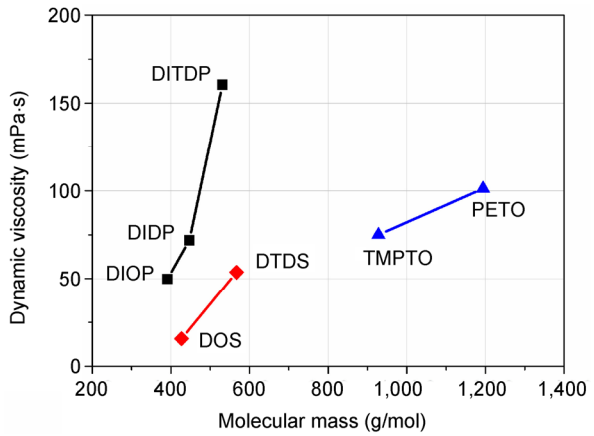

Fig. 2 Ester dynamic viscosity as a function of molecular mass at T = 303 K.

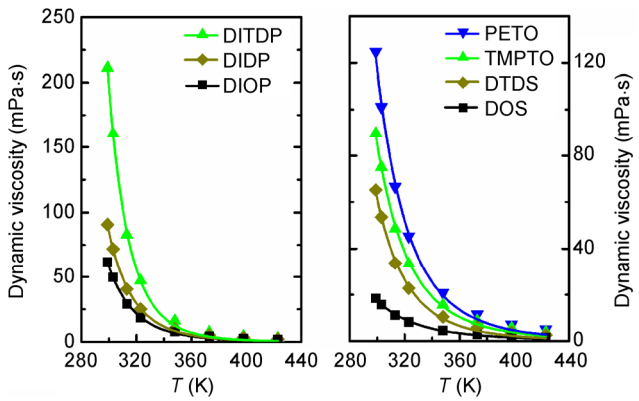

Fig. 3 Ester dynamic viscosity as a function of temperature, obtained through the non-linear regression with Eq. (3).

TMPTO, despite an extra oleate group. This is partly due to the flexibility of the oleate group. A similar phenomenon was also found for polymerized polydimethylsiloxanes (PDMS) [5]. In general, a higher activation energy corresponds to a stronger dependence of viscosity on temperature, suggesting a low viscosity index (VI). Actually, compared with sebacates and polyol esters, phthalates have higher activation energy but lower VI.

3.2 Film thickness

The lubricant film thickness as a function of entrainment speed at three temperatures for the ester samples was measured with the PCS EHD instrument. The Hamrock–Dowson equation (Eq. (1)) was also implemented to calculate the film thickness. The pressure–viscosity index (PVI) values, i.e., Blok's reciprocal asymptotic isoviscous pressure coefficients (α^*) of DIOP and DOS were calculated with the ASME data by Eq. (4) [35–37]

$$\alpha^* = \left[\int_0^\infty \frac{\eta(P=0)\mathrm{d}P}{\eta(P)}\right]^{-1} = \left[\frac{\eta_0}{\alpha_N \eta_N} + \sum_{i=1}^{N} \frac{\eta_0}{\alpha_i} \frac{\eta_i - \eta_{i-1}}{\eta_i \eta_{i-1}}\right]^{-1} \tag{4}$$

where η_i is viscosity at pressure P_i and $\alpha_i = \dfrac{\ln(\eta_i / \eta_{i-1})}{P_i - P_{i-1}}$.

α_N and η_N are the PVI and viscosity at the N-th pressure, respectively. Based on the above results, α^* at different temperature was estimated with the kinematic viscosity at the corresponding temperatures by Eq. (5) [5, 38–40], where m and n are constants.

$$\alpha^* = m \cdot \log(v) + n \tag{5}$$

α^* values for other samples were calculated with the modification of the Hamrock–Dowson method by the Yokoyama-Spikes equation (Eq. (6))

$$\alpha_\mathrm{t} = \alpha_\mathrm{r} \cdot \left(\frac{h_\mathrm{t}}{h_\mathrm{r}}\right)^{1.89} \left(\frac{\eta_\mathrm{r}}{\eta_\mathrm{t}}\right)^{1.26} \tag{6}$$

where subscripts t and r represent a test fluid and the reference fluid, respectively; h is the measured film thickness, and η is the dynamic viscosity of the tested fluid [25]. DIOP was employed as a reference fluid due to its wider viscosity range than DOS. The calculated PVI, m and n for each ester base stock are shown in Table 2. For TMPTO, the PVI values calculated from this work are very close to those from high-pressure viscometer tests (Table 3), suggesting acceptable PVI data from EHD measurements.

For the phthalates from DIOP to DIDP and DITDP, the increase in the length of the hydrocarbon chain

Table 2 Pressure–viscosity indices α^*, refractive index and constants from Eq. (5) of the tested lubricants.

Sample	Pressure-viscosity indices (GPa^{-1})			Refractive index			Constant	
	303 K	348 K	398 K	303 K	348 K	398 K	m	n
DIOP	20.3	14.0	10.3	1.482	1.464	1.444	7.84	6.90
DIDP	23.9	14.4	10.5	1.482	1.464	1.444	10.1	4.63
DITDP	25.9	14.4	9.2	1.480	1.462	1.442	10.9	1.29
DOS	13.5	10.5	8.5	1.446	1.428	1.408	5.66	6.50
DTDS	18.1	14.6	11.5	1.451	1.433	1.413	5.74	8.05
TMPTO	15.1	11.7	10.1	1.472	1.454	1.434	4.58	6.23
PETO	18.5	16.0	13.9	1.474	1.456	1.436	4.07	10.2

Table 3 Comparison of pressure-viscosity indices for trimethylolpropane ester between obtained from this work and those from the literature.

Temperature (°C)	20	40	60	80	Reference
Kinematic viscosity (mm^2/s)	125.0	53.9	27.5	16.5	
TMPTO	15.8	14.2	12.8	11.8	This work*
TMP-ester	15.5	14.4	13.1	12.2	Ref. [6]

* Calculated from Eq. (5) $\alpha^* = 4.58 \times \log(v) + 6.23$.

attached to the phenyl ring results in an increasing dependence of the PVI on kinematic viscosity (Fig. 4). For DOS and DTDS, the longer chain molecule is responsible for the higher PVI following a similar trend of the PVI dependence on kinematic viscosity. This is also true to TMPTO and PETO. Compared with sebacates and polyol esters, the relative rigid phthalates show a stronger PVI dependence on kinematic viscosity.

For all of the lubricants studied, the lubricant film thicknesses decrease remarkably with rising temperature (Figs. 5, 6 and 7) because of the dependence of viscosity and PVI on temperature.

The measured film thicknesses of all samples are consistent with those calculated by the Hamrock–Dowson equation which follow a logarithmic slope of 0.67 versus entrainment speed, suggesting strong Newtonian behaviors. However, at 303 K and high speed ($\geqslant$ 3 m/s), nearly all esters exhibit shear-thinning, especially for PETO and TMPTO, for which shear-thinning appears when the speed is up to 1 m/s.

3.3 Coefficient of friction (COF)

Figure 8(a) shows the variation of the TMPTO lubricant film thickness as a function of entrainment speed at 303, 348, and 398 K, while Fig. 8(b) shows the variation of COF as a function of entrainment speed at 303, 348, and 398 K for the same lubricant at $\Sigma = 0.5$. These two datasets are cross-plotted to generate the plot of COF versus lubricant film thickness shown in Fig. 8(c). At 303 K, the COF shows a weak dependence on the lubricant film thickness, suggesting an adsorbed layer with sufficient asperity protection. Such an adsorbed layer must have been weakly bound, as hinted from the substantially larger COF at the nanoscale film thickness when the temperature increases to 348 and 398 K.

The transition from mixed to full-film lubrication is clearly observed from Fig. 8(c). For example, at 398 K, the COF is about 0.04 at the nearly zero film thickness, dropping rapidly to about 0.01 at roughly 30-nm film thickness, which is about at the same order of

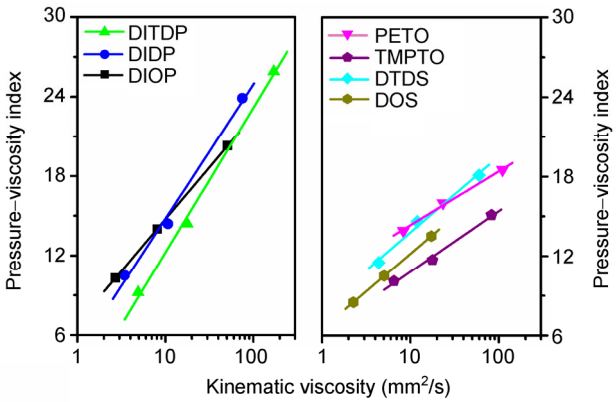

Fig. 4 Pressure–viscosity indices versus kinematic viscosity for DIOP (■), DIDP (●), DITDP (▲), DOS (⬢), DTDS (◆), TMPTO (⬟), and PETO (▼), respectively.

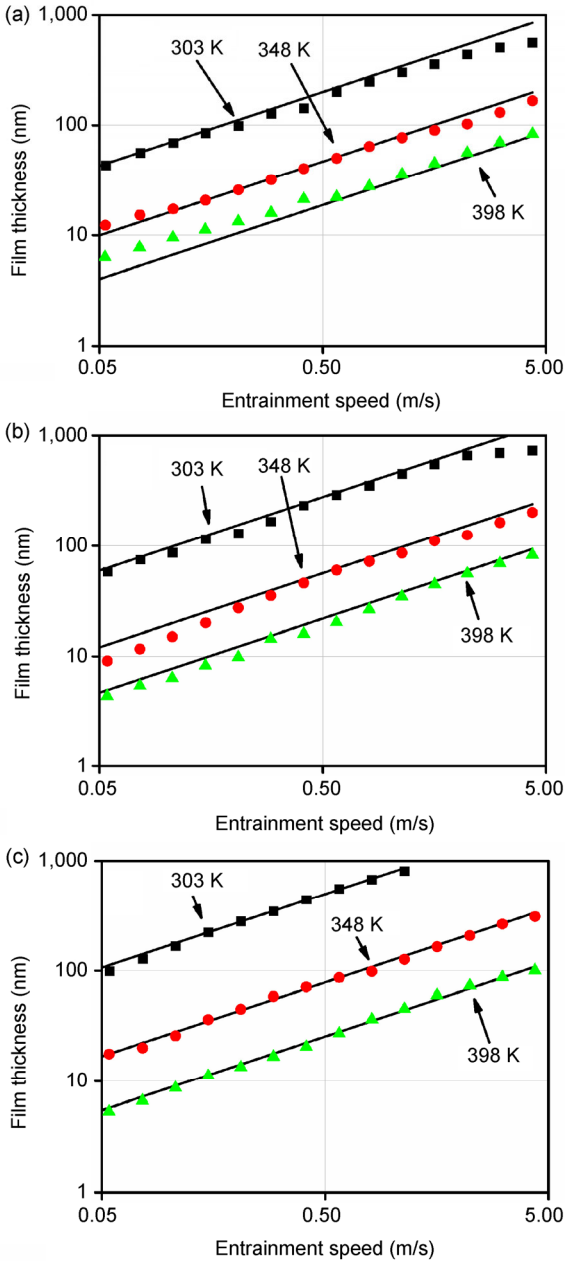

Fig. 5 Measured (symbols) and calculated (lines) film thickness versus entrainment speed for (a) DIOP, (b) DIDP, and (c) DITDP at 303 K (squares), 348 K (circle), and 398 K (triangles).

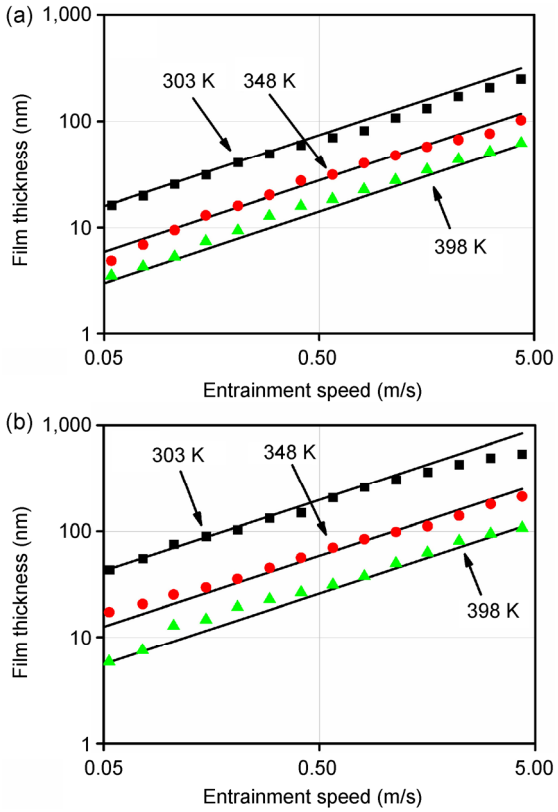

Fig. 6 Measured (symbols) and calculated (lines) film thickness versus entrainment speed for (a) DOS, and (b) DTDS at 303 K (squares), 348 K (circle), and 398 K (triangles).

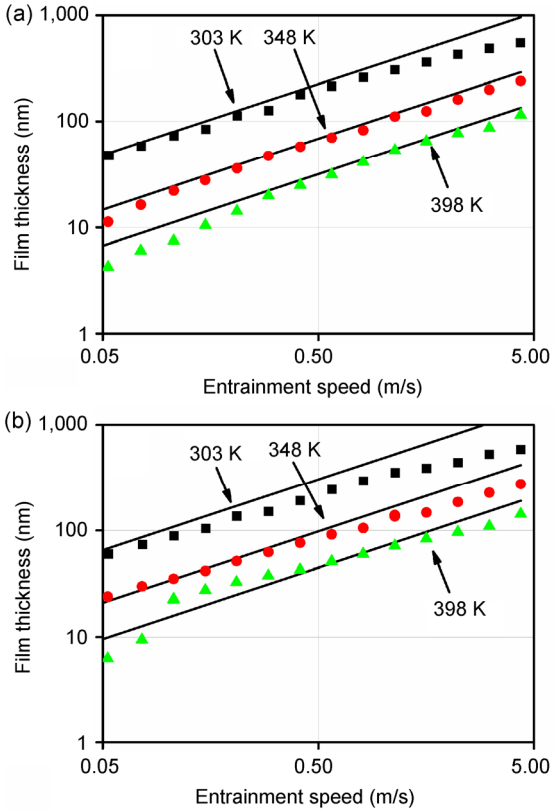

Fig. 7 Measured (symbols) and calculated (lines) film thickness versus entrainment speed for (a) TMPTO, and (b) PETO at 303 K (squares), 348 K (circle), and 398 K (triangles).

magnitude as the composite roughness of the ball–disk interface. This is the film thickness below which the contacting asperities bear a significant portion of the load [22]. For the cases of the same film thickness in the full-film lubrication regime, operation at a higher temperature results in a lower viscosity, and hence a lower COF, as observed. Similar trends can be observed from the data for other samples explored in the present study.

Figure 9 shows the friction coefficient variation as a function of film thickness for DIOP, DIDP, and DITDP at different temperature and $\Sigma = 0.5$. As the speed decreases and thus the film thickness decreases, the contact enters the mixed lubrication regime and the COF starts to rise. At a very slow speed and high temperature (398 K), the film thickness generated is so thin (Fig. 9) that effectively most of the load is borne by solid–solid contact and thus boundary lubrication. The transition from high (mixed lubrication) to low coefficient of friction (full-film lubrication) occurs at around the composite roughness of the ball–disk interface; the friction behavior in the full-film regime is consistent with the bulk viscosity of the lubricants.

In the full-film lubrication regime, the COF of DITDP is the highest while that of DIOP is the lowest at the same film thickness and same temperature. Increasing the length of side chain attached to the phenyl ring has a negative effect on reduction of coefficient of friction. However, in boundary lubrication regime, larger molecules have lower COF. This phenomenon also appeared to DOS and DTDS (Fig. 10). However, compared with the results for TMPTO, PETO yields almost the same COF in most lubrication regimes (Fig. 11) in spite of an extra oleate group in its structure.

Table 4 shows the COF of the tested esters at different temperatures and subjected to the lowest and highest speeds with 50% slide-to-roll ratio. Generally, TMPTO and PETO have the best lubrication performances in both mixed and full-film lubrication regimes.

3.4 Pin-on-disc tests

Coefficients of friction were also measured with the

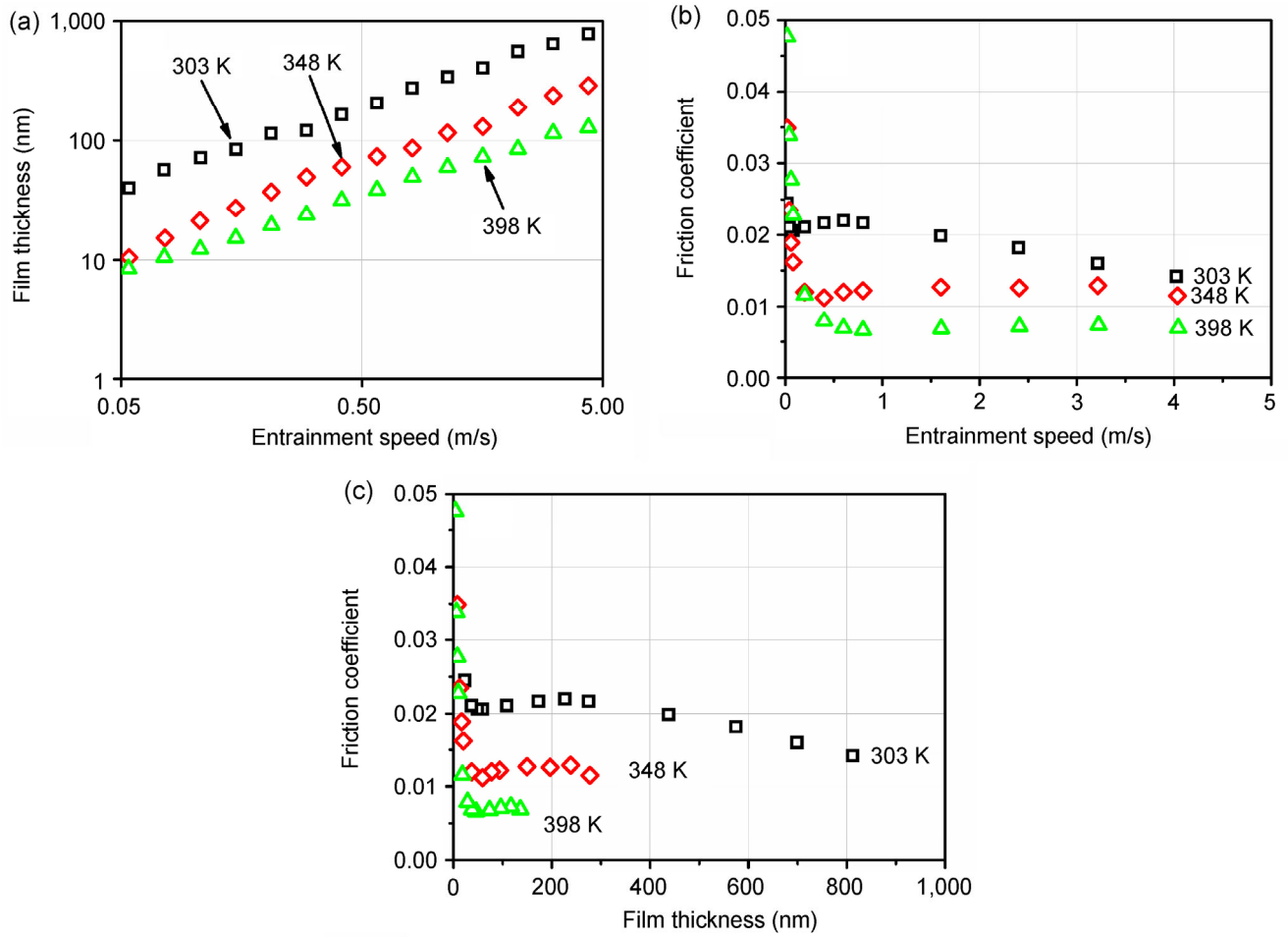

Fig. 8 TMPTO: (a) lubricant film thickness versus entrainment speed at $\Sigma = 0.5$; (b) coefficient of friction versus entrainment speed at $\Sigma = 0.5$; (c) coefficient of friction versus film thickness at $\Sigma = 0.5$ and 303 K (squares), 348 K (diamonds), and 398 K (triangles).

Table 4 Coefficients of friction of esters at the lowest and highest entrainment speeds and different temperatures at $\Sigma = 0.5$.

Sample	0.02 m/s			4.0 m/s		
	303 K	348 K	398 K	303 K	348 K	398 K
DIOP	0.0581	0.0693	0.0938	0.0308	0.0272	0.0106
DIDP	0.0679	0.0751	0.0955	0.0287	0.0333	0.0176
DITDP	0.0721	0.0703	0.0853	0.0225	0.0373	0.0219
DOS	0.0443	0.0761	0.0987	0.0188	0.0101	0.0057
DTDS	0.0539	0.0606	0.0689	0.0251	0.0201	0.0093
TMPTO	0.0245	0.0349	0.0477	0.0142	0.0115	0.0069
PETO	0.0219	0.0251	0.0398	0.0131	0.0118	0.0067

CETR pin-on-disc tribometer at ambient temperature under two speeds, 1.5 mm/s and 150 mm/s of the disc to further confirm the understanding obtained from the film thickness tests. It is observed that an increase in sliding speed leads to a considerable decrease in COF (Fig. 12). Hamrock–Dowson equation (Eq. (1)) was employed to estimate the film thickness. If the interfaces are absolutely smooth, the estimated film thicknesses at 1.5 mm/s for all samples are only several nanometers. It is smaller than the actual composite

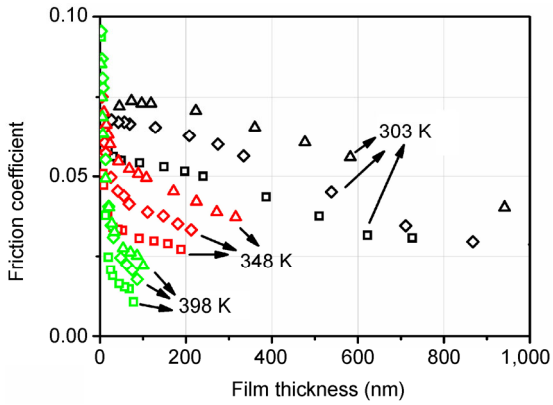

Fig. 9 Coefficient of friction versus film thickness for DIOP (squares), DIDP (diamonds), and DITDP (triangles) at $\Sigma = 0.5$ and 303 K (black), 348 K (red), and 398 K (green).

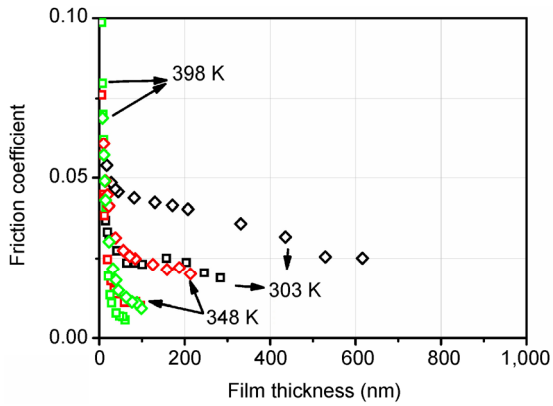

Fig. 10 Coefficient of friction versus film thickness for DOS (squares) and DTDS (diamonds) at $\Sigma = 0.5$ and 303 K (black), 348 K (red), and 398 K (green).

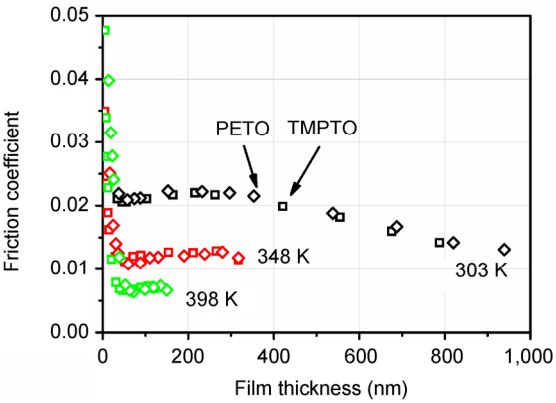

Fig. 11 Coefficient of friction versus film thickness for TMPTO (squares) and PETO (diamonds) at $\Sigma = 0.5$ and 303 K (black), 348 K (red), and 398 K (green).

roughness, suggesting a boundary lubrication regime. At 150 mm/s, the film thickness for DOS is about 29 nm (mixed lubrication regime), and the film thicknesses

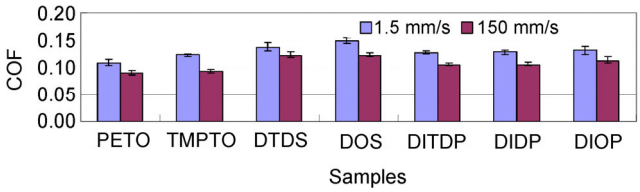

Fig. 12 Coefficient of friction versus velocity for different samples.

of the other six esters are in the range of 80 ~ 213 nm, which implies elastohydrodynamic lubrication. At the lower speed (1.5 mm/s), i.e., in the boundary lubrication regime, the COFs of the three phthalates are very close to each other. Although the phthalates have side chains of different lengths attached to the phenyl ring, the rigid phenyl ring should play a dominant role. For more flexible molecules, such as DOS and DTDS, the increase in chain length induces COFs to decrease. Compared with TMPTO, the extra oleate group of PETO also reduces the COF at the low speed. For relatively flexible structures, the increase in chain length and number of branches can help reduce the COF in the boundary lubrication regime.

It is known that the friction performance depends on several variables, such as the lubricants used, the operating conditions, and the kinematic conditions, such as slip, spin, and side slip [41]. Although there are differences between the EHL friction tester and pin-on-disc tester, a comparison is still helpful. The trend of the pin-on-disc test results at the low speed is similar to that in the EHL friction tests (Table 4). At 0.02 m/s and 398 K, i.e., in the mixed/boundary lubrication regime, longer chains and more branches facilitate COF reduction. However, at this high temperature, DTDS shows a lower COF than DITDP does although they have the same two isotridecyl groups and similar molecular weight. This implies that the flexible molecules more readily decrease in COF at a high temperature.

At 150 mm/s, i.e., in the elastohydrodynamic lubrication regime, PETO and TMPTO have the lowest COF. The increase in chain length and number of branches also result in a slight reduction of COF at high speed. This trend can be also found in the EHL friction results (Table 4), at 4.0 m/s and 303 K, i.e., in the elastohydrodynamic/hydrodynamic lubrication regime. From DIOP to DIDP and DITDP, the increase

in the chain length on the phenyl ring yields a benign COF drop. Compared with TMPTO, PETO shows a lower COF induced by an extra oleate group. Polyol esters also show the lowest COF here. These may be partly attributed to temporary shear thinning at high speed. With increasing slide-to-roll ratio from $\Sigma = 0$ to $\Sigma = 0.5$ and to $\Sigma = 1$, i.e., with increasing shear stress, the film thickness of PETO decreases, especially at high speed (Fig. 13). Similar phenomena also appear to the other tested ester base stocks.

However, for DOS and DTDS, although DTDS also show a temporary shear thinning, its COF is a little larger than that of DOS, partly owing to its higher viscosity (three times as that of DOS); viscosity plays a dominant role in this case.

Combining the EHL friction and pin-on-disc results reveals that polyol esters like TMPTO and PETO have the best lubricating performance among all the tested ester base stocks at boundary, mixed, and full-film lubricating regimes. The polar ester group plays an important role because it can be adsorbed by the polar interface. Therefore, more ester groups in one molecule can provide stronger attachment to surfaces, which renders a more efficient antifriction ability of the lubricant. At low temperature, the relatively rigid molecules like phthalates show better friction performance in the boundary lubrication regime than do the flexible sebacates whose molecules have nearly the same number of carbon atoms as phthalates. Rigid molecules have strong anti-transformation ability under pressure, so that they may provide more effort to separate the contact interfaces. On the contrary, at a high temperature, rigid phthalate molecules have a negative impact on COF reduction in the boundary lubrication regime.

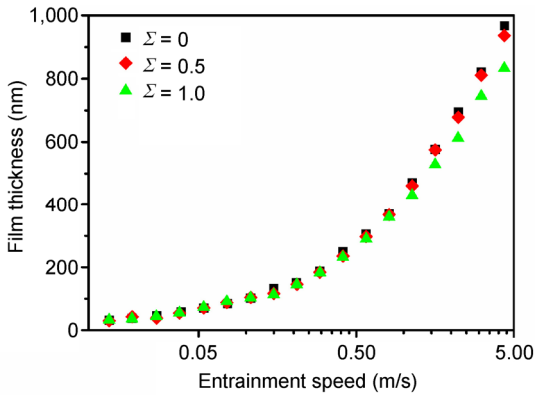

Fig. 13 Film thickness versus entrainment speed for PETO at 303 K and different slide-to-roll ratio $\Sigma = 0$ (squares), 0.5 (diamonds), and 1.0 (triangles).

4 Conclusions

The present work explored lubrication properties of ester base stocks through investigations of the relationships among molecular structure, viscosity, film formation, and coefficients of friction. The results reveal that the tested samples exhibit diverse lubrication performance due to the differences in chain length, geometric configuration, and rigidity or flexibility of the molecular structures.

(1) Density decreases and viscosity increases with increases of the hydrocarbon chain length for the phthalates and sebacates. The addition of the oleate group, from TMPTO to PETO, causes the increases in both density and viscosity. The phenyl group increases the sensitivity of both the viscosity and pressure-viscosity coefficient to temperature change.

(2) For all ester base stocks tested, the lubricant film thickness decreases with increasing temperature, and the relationship between film thickness and entrainment speed implies a Newtonian behavior. However, at low temperature and high speed, PETO and TMPTO exhibit obvious shear thinning behavior.

(3) For the phthalates and sebacates, while they have the same film thickness, the increase in chain length negatively affects coefficients of friction in the full-film lubrication regime, opposite to their behaviors in the mixed lubrication regime at $\Sigma = 0.5$ and 398 K. However, for the polyol esters from TMPTO to PETO, the coefficients of friction show a weak dependence on molecular size in most of the lubrication regimes. Comparatively, the polyol esters demonstrate better lubrication properties.

Acknowledgements

Yifeng He and Yuzhen Zhao would like to acknowledge the support from Visiting Scholar Project of China Petrochemical Corporation (Sinopec). The authors would like to thank Center for Surface Engineering and Tribology at Northwestern University, USA, for research support. The Northwestern authors would

also like to acknowledge the support from US Department of Energy (DE-EE0006449). The views and opinions of authors expressed herein do not necessarily state or reflect those of the United States Government or any agency thereof.

References

[1] Sharma S K, Snyder C E, Gschwender L J. Tribological behavior of some candidate advanced space lubricants. *Tribol Trans* **36**(2): 321–325 (1993)

[2] Ziegler M, Fearon F. Silicon-based polymer science: A comprehensive resource. In *Advances in Chemistry Series*. Washington, DC: American Chemical Society, 1990.

[3] De Jaeger R, Gleria M. *Inorganic Polymers*. New York: Nova Science Publishers Inc., 2007.

[4] Schneider M P. Plant-oil-based lubricants and hydraulic fluids. *J Sci Food Agr* **86**(12): 1769–1780 (2006)

[5] Zolper T J, Li Z, Chen C L, Jungk M, Marks T J, Chung Y W, Wang Q. Lubrication properties of polyalphaolefin and polysiloxane lubricants: Molecular structure-tribology relationships. *Tribol Lett* **48**(3): 355–365 (2012)

[6] Höglund E. Influence of lubricant properties on elastohydrodynamic lubrication. *Wear* **232**(2): 176–184 (1999)

[7] Foord C A, Hammann C W, Cameron A. Evaluation of lubricants using optical elastohydrodynamics. *Tribol Trans* **11**(1): 31–43 (1968)

[8] Gohar R, Cameron A. Mapping of elastohydrodynamic contacts. *ASLE Trans* **10**(3): 215–225 (1967)

[9] Spikes H A, Cann P M. The development and application of the spacer layer imaging method for measuring lubricant film thickness. *Proc IMechE, Part J: J Eng Tribol* **215**(3): 261–277 (2001)

[10] Molimard J, Querry M, Vergne P. New tools for the experimental study of EHD and limit lubrications. *Tribol S* **36**: 717–726 (1999)

[11] Hamrock B J, Dowson D. *Ball Bearing Lubrication: The Elastohydrodynamics of Elliptical Contacts.* Lewis Research Center, Cleveland: National Aeronautics Space Administration, 1981.

[12] Guangteng G, Spikes H A. Boundary film formation by lubricant base fluids. *Tribol Trans* **39**(2): 448–454 (1996)

[13] Smeeth M, Spikes H A, Gunsel S. The formation of viscous surface films by polymer solutions: Boundary or elastohydrodynamic lubrication. *Tribol Trans* **39**(3): 720–725 (1996)

[14] Bair S, Winer W O. A simple formula for EHD film thickness of non-Newtonian liquids. *Tribol S* **32**: 235–241 (1997)

[15] Aderin M, Johnston G J, Spikes H A, Caporiccio G. The elastohydrodynamic properties of some advanced nonhydrocarbon-based lubricants. *Lubr Eng* **48**(8): 633–638 (1992)

[16] Guangteng G, Spikes H A. The control of friction by molecular fractionation of base fluid mixtures at metal surfaces. *Tribol Trans* **40**(3): 461–469 (1997)

[17] Bair S. Elastohydrodynamic film forming with shear thinning liquids. *J Tribol—Trans ASME* **120**(2): 173–178 (1998)

[18] Dyson A, Wilson A. Paper 3: Film thicknesses in elastohydrodynamic lubrication by silicone fluids. Proceedings of the Institution of Mechanical Engineers, Conference Proceedings: SAGE Publications, 1965: 97–112.

[19] Johnston G J, Wayte R, Spikes H A. The measurement and study of very thin lubricant films in concentrated contacts. *Tribol Trans* **34**(2): 187–194 (1991)

[20] Bair S, Qureshi F. The generalized newtonian fluid model and elastohydrodynamic film thickness. *J Tribol—Trans ASME* **125**(1): 70–75 (2003)

[21] Bair S. A rough shear-thinning correction for EHD film thickness. *Tribol Trans* **47**(3): 361–365 (2004)

[22] Gunsel S, Korcek S, Smeeth M, Spikes H A. The elastohydrodynamic friction and film forming properties of lubricant base oils. *Tribol Trans* **42**(3): 559–569 (1999)

[23] Chang H S, Spikes H A, Bunemann T P. The shear stress properties of ester lubricants in elastohydrodynamic contacts. *J Syn Lubr* **9**(2): 91–114 (1992)

[24] Fernández J, Luque P, Cuervo D. Influence of load and lubricants on EHD film thickness and rolling-contact fatigue lives of AISI 52100 steel balls. *J Syn Lubr* **15**(4): 293–309 (1999)

[25] Yokoyama F, Spikes H A. Film-forming properties of polyol esters, polyphenyl ethers and their mixtures over a wide range of temperature. *Tribol Trans* **43**(1): 130–136 (2000)

[26] Larsson R, Kassfeldt E, Byheden Å, Norrby T. Base fluid parameters for elastohydrodynamic lubrication and friction calculations and their influence on lubrication capability. *J Syn Lubr* **18**(3): 183–198 (2001)

[27] Lord J, Larsson R. Effects of slide-roll ratio and lubricant properties on elastohydrodynamic lubrication film thickness and traction. *Proc IMechE, Part J: J Eng Tribol* **215**(3): 301–308 (2001)

[28] Biresaw G, Sharma B K, Bantchev G B, Kurth T L, Doll K M, Erhan S Z, Kunwar B, Scott J W. Elastohydrodynamic properties of biobased heat-bodied oils. *Ind Eng Chem Res* **53**(42): 16183–16195 (2014)

[29] Biresaw G, Cermak S C, Isbell T A. Film-forming properties of estolides. *Tribol Lett* **27**(1): 69–78 (2007)

[30] Bantchev G B, Biresaw G, Cermak S C. Elastohydrodynamic study of blends of bio-based esters with polyalphaolefin in the low film thickness regime. *J Am Oil Chem Soc* **89**(6): 1091–1099 (2012)

[31] Bantchev G B, Biresaw G. Film-forming properties of castor oil-polyol ester blends in elastohydrodynamic conditions. *Lubr Sci* **23**(5): 203–219 (2011)

[32] Sarpal A, Sastry M, Kumar R, Bhadhavath S, Rai K, Bansal V, Patel M. Molecular dynamics of synthetic-based lubricant system by spectroscopic techniques—Part 1. *Tribol Trans* **56**(3): 442–452 (2013)

[33] Roelands C J A. Correlational aspects of the viscosity-temperature-pressure relationship of lubricating oils: TU Delft, Delft University of Technology, 1966.

[34] Vankrevelen D W, Hoftyzer P J. Newtonian shear viscosity of polymeric melts. *Angewandte Makromolekulare Chemie* **52**(1): 101–109 (1976)

[35] Bair S, Qureshi F. Accurate measurements of pressure-viscosity behavior in lubricants. *Tribol Trans* **45**(3): 390–396 (2002)

[36] Ramasamy U S, Bair S, Martini A. Predicting pressure–viscosity behavior from ambient viscosity and compressibility: challenges and opportunities. *Tribol Lett* **57**(2): 1–7 (2015)

[37] *ASME: Pressure-viscosity Report*. New York: American Society of Mechanical Engineers, 1953.

[38] Schrader R. *Zur Schmierfilmbildung von Schmierolen und Schmierfetten im elastohydrodynamischen Walzkontakt*. Dissertation, Hannover, 1988.

[39] Gold P, Schmidt A, Dicke H, Loos J, Assmann C. Viscosity–pressure–temperature behaviour of mineral and synthetic oils. *J Syn Lubr* **18**(1): 51–79 (2001)

[40] Ohno N, Mia S, Morita S, Obara S. Friction and wear characteristics of advanced space lubricants. *Tribol Transs* **53**(2): 249–255 (2010)

[41] Muraki M, Sakaguchi K. Influence of the size, geometry, and material of the rollers on EHD traction. *J Syn Lubr* **9**(3): 205–221 (1992)

Yifeng HE. He received his B.S. and Ph.D degrees in applied chemistry from Peking University, Beijing, in 2003 and 2009 respectively. During his postgraduate period, he studied in the Department of Chemistry at Moscow State University, Russia, during 2004 and 2005. He joined Sinopec Research Institute of Petroleum Processing in 2009, and now is a senior research engineer. From 2014 to 2015, he was a visiting scholar in the Center for Surface Engineering and Tribology at Northwestern University, USA. His research interests are in the development of lubricating oils and greases, and investigation on their lubrication properties and tribological behaviours.

Qian WANG. She received her Ph.D degree from Northwestern University, USA, 1993. She taught for five years at Florida International University, Miami, FL, USA, and is now a professor in the Mechanical Engineering Department at Northwestern University, USA. Her research interests are in theories and modelling of tribological interfaces and developments of robust and energy effective tribological systems. She received the International Award from Society of Tribologists and Lubrication Engineers (STLE) in 2015; she was elected Fellow of the American Society of Mechanical Engineers (ASME) in 2009 and STLE in 2007.